NeuroImage 209 (2020) 116477

Contents lists available at ScienceDirect

NeuroImage

journal homepage: www.elsevier.com/locate/neuroimage

Prenatal exposure to maternal cigarette smoking and structural properties of the human corpus callosum

L. Björnholm [a,*], J. Nikkinen [b,c], V. Kiviniemi [d,e], S. Niemelä [f,g], M. Drakesmith [h], J.C. Evans [h], G.B. Pike [i], L. Richer [j], Z. Pausova [k,l], J. Veijola [a], T. Paus [m,n,**]

[a] Department of Psychiatry, Research Unit of Clinical Neuroscience, University of Oulu and Oulu University Hospital, Oulu, Finland
[b] Department of Radiotherapy, Oulu University Hospital, Oulu, Finland
[c] MIPT/MRC, University of Oulu and Oulu University Hospital, Oulu, Finland
[d] Institute of Diagnostics, Department of Diagnostic Radiology, Oulu University Hospital, Oulu, Finland
[e] Oulu Functional Neuroimaging, MIPT/MRC, University of Oulu and Oulu University Hospital, Oulu, Finland
[f] Department of Psychiatry, University of Turku, Turku, Finland
[g] Addiction Psychiatry Unit, Department of Psychiatry, Hospital District of Southwest Finland, Finland
[h] School of Psychology, Cardiff University, Cardiff, United Kingdom
[i] Department of Radiology and Clinical Neurosciences, University of Calgary, Calgary, AB, Canada
[j] Department of Health Sciences, Université du Québec à Chicoutimi, Chicoutimi, QC, Canada
[k] The Hospital for Sick Children, University of Toronto, Toronto, ON, Canada
[l] Departments of Physiology and Nutritional Sciences, University of Toronto, Toronto, ON, Canada
[m] Bloorview Research Institute, Holland Bloorview Kids Rehabilitation Hospital, Toronto, Canada
[n] Departments of Psychology and Psychiatry, University of Toronto, Toronto, Canada

A B S T R A C T

Alterations induced by prenatal exposure to nicotine have been observed in experimental (rodent) studies. While numerous developmental outcomes have been associated with prenatal exposure to maternal cigarette smoking (PEMCS) in humans, the possible relation with brain structure is less clear. Here we sought to elucidate the relation between PEMCS and structural properties of human corpus callosum in adolescence and early adulthood in a total of 1,747 youth. We deployed three community-based cohorts of 446 (age 25–27 years, 46% exposed), 934 (age 12–18 years, 47% exposed) and 367 individuals (age 18–21 years, 9% exposed). A mega-analysis revealed lower mean diffusivity in the callosal segments of exposed males. We speculate that prenatal exposure to maternal cigarette smoking disrupts the early programming of callosal structure and increases the relative portion of small-diameter fibres.

1. Introduction

Cortico-cortical connections are formed in the early fetal period (McConnell et al., 1989). The development of axonal connections is guided by numerous signaling molecules, making it prone to external insults (Lauder, 1985). Prenatal exposure to maternal cigarette smoking (PEMCS) exposes the fetus to hypoxia and a large number of chemicals including nicotine (Luck et al., 1985), which is a potent neuromodulator due to the early expression of nicotinic receptors in the developing brain (Atluri et al., 2001). Numerous studies have reported disrupted neural development due to *in utero* exposure to nicotine in experimental animals (Ernst et al., 2001). Nicotine causes abnormalities in cell proliferation and differentiation (Slotkin et al., 1986), alters neuronal pathfinding (Zheng et al., 1994), and disrupts the development of the cholinergic and catecholaminergic systems (Oliff and Gallardo, 1999) as well as the functions of sex hormones (Lichtensteiger and Schlumpf, 1985). Many alterations caused by prenatal exposure to nicotine persist after birth (Slotkin et al., 1986, 1987) or may emerge later in development due to modified genetic programming (Yochum et al., 2014).

Prenatal exposure to maternal cigarette smoking is one of the most prevalent harmful prenatal factors in industrialized countries; globally, more than half of women who smoke daily continue smoking during pregnancy (Lange et al., 2018). In large observational studies, this exposure has been associated with various detrimental outcomes at birth or later in life. The former includes lower birth weight (D'Onofrio et al., 2003) and smaller head circumference (Källén, 2000), while the latter includes overweight (Albers et al., 2018), lower cognition (Fried, 1995) and poor mental health (Wakschlag et al., 2002). The causality of these

* Corresponding author. Department of Psychiatry, University of Oulu, Oulu, 90014, Finland.
** Corresponding author. Bloorview Research Institute, Toronto, M4G 1R8, Canada.
E-mail addresses: lassi.bjornholm@oulu.fi (L. Björnholm), tpaus@hollandbloorview.ca (T. Paus).

https://doi.org/10.1016/j.neuroimage.2019.116477
Received 18 January 2019; Received in revised form 9 December 2019; Accepted 18 December 2019
Available online 24 December 2019

(and other) associations between PEMCS and various possible outcomes is, however, impossible to establish in such observational studies; in many cases, these associations may be due to other (unmeasured) genetic and environmental factors (Ernst et al., 2001; D'Onofrio et al., 2003). In fact, findings in genetically informed studies do not support a causal effect of PEMCS on later development of externalizing disorders or attention deficit hyperactivity disorder (ADHD), but are rather consistent with the effect of inherited or family factors (Gustavson et al., 2017; D'Onofrio et al., 2008).

Brain imaging, not bound by diagnostic criteria, has the potential to help with bridging the gap between preclinical and clinical observations. Based on earlier experimental and observational research, structural alterations in brain associated with PEMCS are likely diverse. Reported associations between PEMCS and imaging measures include reduced head growth in the fetal period (Roza et al., 2007) and smaller total brain and cortical grey-matter volumes in school-aged children (El Marroun et al., 2014). We have previously reported thinner orbitofrontal cortex in both male and female adolescents, and lower size of the corpus callosum in female adolescents with (vs. without) PEMCS (Toro et al., 2008; Paus et al., 2008). Another study on corpus callosum observed an association between PEMCS and higher fractional anisotropy in the anterior corpus callosum in adolescents (Jacobsen et al., 2007). The opposite, namely lower fractional anisotropy in the same callosal region, was observed in another study (Liu et al., 2011). While offering valuable findings, these two studies were limited by relatively small sample size and differences in offspring age.

Corpus callosum is the largest fiber-tract in the human brain, connecting the two brain hemispheres (Aboitiz et al., 1992). Inter-hemispheric transfer of information is reflected in the composition of callosal fibers. We have recently compared structural properties of the corpus callosum, assessed *in vivo* with MRI, with the distribution of large and small caliber fibers, as assessed *in vitro* (Björnholm et al., 2017). In the present report, we focus on an association between maternal smoking during pregnancy and structural properties of the corpus callosum in adolescents and youth drawn from three community-based cohorts. We use six complementary MRI measures sensitive to structural properties of brain tissue: Longitudinal Relaxation Rate (R1 = 1/T1, i.e. the inverse of longitudinal relaxation time), Transverse Relaxation Rate (R2 = 1/T2) and Myelin-Water Fraction (MWF) are sensitive to tissue water and myelin content (MacKay et al., 2006); Magnetization Transfer Ratio (MTR) is a proxy of tissue macromolecular content, and is dominated by myelin in white matter (Sled, 2018; Schmierer et al., 2004); Fractional Anisotropy (FA) and Mean Diffusivity (MD) are measures sensitive to the density, arrangement and morphology of axonal bundles (Mori and Zhang, 2006). Finally, we use callosal mid-sagittal volume as a proxy of the overall morphology and number of callosal fibers (Aboitiz et al., 1992). Based on earlier studies associating PEMCS with disrupted morphology of neural tissue (Ernst et al., 2001), unfavorable neurodevelopmental outcomes (Källén, 2000) and long-term epigenetic variation (Lee et al., 2015), we hypothesize that the composition of callosal fibers is altered in youth exposed prenatally to maternal cigarette smoking, as compared with non-exposed individuals.

2. Materials and methods

2.1. Study setting and analytical approach

The three cohort studies were approved by their local ethics committees and participants (or their guardians) have given written consent to participate in the study. A more detailed description of each study is given in Supplementary Materials and Methods.

In order to evaluate robustness of any PEMCS-associated variations in the structural properties of the corpus callosum, we have designated the NFBC1986 (see below) as a discovery cohort and the SYS and ALSPAC as replication cohorts. The NFBC1986 was chosen because all MRI measures therein can be tested for replication in at least one of the two replication cohorts. In addition, in measures available in two or more cohorts, we provide results of their mega-analysis.

2.1.1. The NFBC 1986 Study

The Northern Finland Birth Cohort 1986 Study (NFBC, 1986; http://www.oulu.fi/nfbc/) is a prospective population-based collection of health-related information about individuals with expected date of birth between the 1st of July 1985 and the 30th of June 1986 in the Northern Finland (Järvelin et al., 1993). A subsample of 698 individuals exposed to maternal smoking during pregnancy (smoking continued during the 2nd trimester) had existing data of a previous follow-up and were eligible for inclusion in the current study. The non-exposed control group was selected randomly from offspring of non-smoking mothers with the same inclusion and exclusion criteria as the exposed group (Lotfipour et al., 2014). The following exclusion criteria were used: participant was adopted, use of alcohol by the mother during pregnancy (excl. >210 ml alcohol/week), diabetes of the mother during pregnancy (onset before pregnancy, treated by insulin), premature birth (<35 weeks) and/or detached placenta, multiple births, hyperbilirubinemia requiring transfusion, type 1 diabetes, systemic rheumatologic disorders, malignant tumors requiring chemotherapy, congenital heart defects or heart surgery, aneurysm, epilepsy, bacterial infection of CNS, brain tumor, head trauma with loss of consciousness > 30 min, muscular dystrophy, myotonic dystrophy, nutritional and metabolic diseases, major neurodevelopmental disorders (e.g. autism), hearing deficit requiring hearing aid, vision problems (strabismus, visual deficit not correctable), treatment for schizophrenia or bipolar disorder, IQ < 70, low reading ability (<2 SD), special education.

Data concerning maternal smoking were collected from two questionnaires, one completed by the mothers during pregnancy and one by midwives right after delivery. The offspring of those women who continued to smoke after the first trimester formed the exposed group. Non-exposed controls were matched to the exposed participants by maternal education (using 5-level categories of basic and occupational education) and place of birth (urban/rural and Oulu/Lapland region). Of the invited 1,396 individuals (698 exposed and 698 matched non-exposed), a total of 471 (34%) participated in the MRI study. Data for callosal volume, FA, MD or MTR were available for 446 individuals (age 25–27 years, mean [SD] = 26.45 [0.51]); 206 individuals (46%) were exposed to maternal smoking during pregnancy.

2.1.2. The SYS

The Saguenay Youth Study (SYS; http://saguenay-youth-study.org) is aimed at evaluating brain and cardiometabolic health during adolescence (Pausova et al., 2007). French-Canadian adolescents, aged 12–18 years (N = 1029; mean age 15.0 ± 1.8 years) were recruited from high schools in the Saguenay/Lac-Saint-Jean region of Quebec, Canada; half of the adolescents were exposed to maternal smoking during pregnancy and the other (non-exposed) half was matched to the exposed by maternal education and school attended. The exposed group included those participants whose mother continued to smoke during the 2nd trimester of pregnancy. The SYS uses a family-based design where two or more siblings from the same family are included. Details of recruitment and testing procedures are provided in (Pausova et al., 2007).

The main exclusion criteria for both exposed and non-exposed adolescents were: (i) premature birth (<35 weeks); (ii) positive history of alcohol abuse during gestation; (iii) positive medical history for meningitis, malignancy, and heart disease requiring heart surgery (iv) severe mental illness (e.g., autism, schizophrenia); or mental retardation (IQ < 70) and (v) MRI contraindications. The Research Ethics Committee of the Chicoutimi Hospital approved the study protocol. Adolescents and their parents signed informed assent and consent, respectively (Pausova et al., 2017).

In the current study, MRI data in callosal volume or MTR were available for 934 individuals (age 12–18 years, mean [Standard Deviation, SD] = 15.02 [1.83]); 442 individuals (47%) were exposed to

maternal smoking during pregnancy. The number of individuals with existing data on each MRI measure is specified in Supplementary Materials and Methods.

2.1.3. The ALSPAC study

The Avon Longitudinal Study of Parents and Children birth cohort was designed to investigate the influence of various factors on health trajectories. Pregnant women residing in the former Avon Health Authority in South-West England, who had an estimated date of delivery between 1 April 1991 and 31 December 1992 were invited to participate in the study. This resulted in a cohort of 14,541 pregnancies, of which 13,988 singletons/twins were alive at 12 months of age (Fraser et al., 2013). Participants of this study were selected from the original cohort (Boyd et al., 2013) based on their current domicile being within a 3-h journey (1-way) from the scanning site and the availability of a minimum of three blood samples obtained for sex-hormone assays (Khairullah et al., 2014). The sample included the first 507 participants who met these criteria and accepted the invitation to take part in the MRI substudy.

Information of maternal smoking was collected from the mothers during pregnancy using questionnaires. Exposure to maternal cigarette smoking during the 2nd trimester was used as criteria for the exposed group and no maternal smoking before or during pregnancy for the non-exposed group. A total of 507 male participants from ALSPAC were scanned. Only male participants were included owing to the focus of the NIH grant funding this work. Data for callosal volume, FA, MD, MTR, R1, R2 or MWF were available for 367 individuals (age 18–21 years, mean [SD] = 19.57 [0.82]); 34 individuals (9%) were exposed to maternal smoking during pregnancy, please see Supplementary material for details on exclusion.

2.2. Image acquisition

All MRI datasets were acquired during a single session in each cohort. Datasets for each cohort included a high-resolution (1-mm isotropic) T1w structural scan and parametric imaging, including Magnetization Transfer Imaging (ALSPAC, SYS and NFBC1986), Diffusion-Weighted Imaging (NFBC1986 and ALSPAC) and Multi-Component Driven Equilibrium Single-Pulse Observation of T1 and T2 (mcDESPOT; ALSPAC). Data were acquired using equipment and parameters detailed in Table 1.

2.3. Image processing

All MRI data (ALSPAC, SYS and NFBC1986) were processed on a scientific cluster environment (*Taito*, CSC) using the most recent versions of identical software and processing configuration in all cohorts. Ten callosal segments were drawn on the MNI152 1-mm brain template as explained in (Björnholm et al., 2017). The segments were then transformed nonlinearly into native T1w images. Parametric images were also transformed into native T1w images, where mean and volumetric parameters of callosal segments were automatically extracted (ALSPAC: segment volume, FA, MD, MTR, R1, R2 and MWF; SYS: segment volume and MTR; NFBC1986: segment volume, FA, MD and MTR), see below for details for each imaging modality.

First, T1-weighted (T1w) scans were stripped of non-brain tissue using *bet* (T2: based estimation, 2005), and the resulting brain was registered linearly (brain-only, *flirt*, 12 dof) and nonlinearly (whole-head, *fnirt*) to the MNI152 1-mm template (Andersson et al., 2007; Jenkinson and Smith, 2001). Callosal segments in the MNI152 1-mm template were then back-projected to native T1w images using information from this registration.

In order to enhance the quality of the projection of the segments in the SYS sample (age 13-18-y), an additional registration to a SYS808 template was performed (note that MNI152 is based on adult scans). This included linear and nonlinear registration of each individual's T1w image to the SYS808 1-mm template (created by nonlinear averaging of T1w images of a subset of SYS participants), and a registration of the SYS808 template to the MNI152 template (linear and nonlinear). Callosal segments in the SYS sample were then back-projected in one interpolation step from the MNI152 template, *via* the SYS808 template, to the native T1w images.

2.3.1. Callosal segment volume

In order to account accurately for the inter-individual variation in callosal morphology, a different procedure was used for extracting the

Table 1
Parameters of acquisition of brain MRI. a) T1-weighted (T1w) and Magnetization Transfer Imaging (MTI) in the Saguenay youth Study (SYS) and T1w, Diffusion-Weighted Imaging (DWI) and MTI in the Northern Finland Birth Cohort 1986 (NFBC1986) and the Avon Longitudinal Study of Parents and Children (ALSPAC). b) Acquisition parameters for Multi-Component Driven Equilibrium Single-Pulse Observation of T1 and T2 (mcDESPOT) in ALSPAC.

a)	The NFBC1986 Study[a]			The SYS Study[b]			The ALSPAC Study[c]		
Modality	T1w	DWI	MTI	T1w	MTI	MTI	T1w	DWI	MTI
Repetition time (ms)	2400	9000	30	25	41	30	7.9	cardiac-gated	26.7
Echo time (ms)	2.56	102	11	4.2	7.9	11	3	87	1.8
Flip angle (°)	8	90	15	30	30	15	20	90	5
Resolution (mm, x/y/z)	1/1/1	2.3/2.3/2.3	1/1/3	1/1/1	1/1/3	1/1/3	1/1/1	2.4/2.4/2.4	1.9/1.9/1.9
Other parameters	TI = 1000 ms	64 (b = 1000 s/mm^2) + 1 (b = 0 s/mm^2)	1.5 kHz and 500 deg[e]	–	1.5 kHz and 500 deg[e]	1.5 kHz and 500 deg[e]	TI = 450 ms	30 (b = 1200 s/mm^2) + 3 (b = 0 mm/s^2)	2 kHz and 450 deg[e]

b)	The ALSPAC Study: T1, T2 and MWF (mcDESPOT)[d]		
Modality	SPGR	IR-SPGR	SSFP
Repetition time (ms)	4.7	4.7	3.2
Echo time (ms)	2.112	2.112	1.6
Flip angle (°)	3, 4, 5, 6, 7, 9, 13 and 18	5	10.59, 14.12, 18.53, 23.82, 29.12, 35.29, 45 and 60
Resolution (mm, x/y/z)	1.72/1.72/1.72	1.72/1.72/1.72	1.72/1.72/1.72
Other parameters	–	IR = 450 ms	Phase-cycling angles of 0° and 180°

[a] 1.5 T S Magnetom Espree scanner using sequences: gradient recalled inversion recovery spoiled magnitude prepared oversampling phase 3D (T1w), spin-echo echo-planar (DWI) and spoiled gradient recalled 3D (MTI).
[b] 1.0 T Philips scanner using sequences: 3D radio frequency-spoiled gradient echo (T1w) and 3D T1 Fast Field Echo (MTI).
[c] 3.0 T General Electric HDx scanner using sequences: 3D fast spoiled gradient recall (T1w), dual spin-echo, single shot echo-planar imaging with zero-filling to 1.8 × 1.8 × 2.4 mm resolution (DWI), 3D spoiled gradient recalled (MTI) and 3D fast spoiled gradient recall (mcDESPOT).
[d] Acquisition included 8 T1-weighted spoiled gradient recalled echo (SPGR) images, 2 inversion-prepared SPGR images (IR-SPGR) and 15 T1/T2 weighted steady-state free precession (SSFP) images (eight flip angles, two phase-cycling angles).
[e] RF saturation frequency offset and flip angle.

volumetric data. First, the 10 callosal segments in the MNI152-1 mm template were expanded to the outermost outline of the corpus callosum on two midsagittal slices. The segments were then projected to the native T1w space using the same registrations as above. Second, in each individual, brain tissue classified as white matter with at least 95% probability in *fsl fast* was used for masking the callosal segments in native space. Finally, masked segments were inspected visually and volumes extracted automatically.

2.3.2. Diffusion-weighted images

Non-diffusion-weighted b0 scans were stripped of non-brain tissue using *bet*, after which the three b0 scans in the ALSPAC sample were aligned (*flirt*, 6 dof) and averaged. The data were corrected for head motion, eddy-currents, slice-wise outliers and within-volume motion in *FSL eddy cuda 8.0* (Andersson and Sotiropoulos, 2016) using parameters *repol* (Andersson et al., 2016) and *mporder=4* (Andersson et al., 2017). Parametric FA and MD maps were then calculated in *dtifit* using rotated b-vectors. To minimize the effect of echo-planar imaging (EPI) artefacts (Irfanoglu et al., 2012), the FA images were eroded to eliminate bright edges using *fslmaths* and linearly (brain-only, *flirt*, 12 dof) and non-linearly (brain-only, *fnirt*) registered to the native T1w images. Distortions in the MD images were corrected using the same transformations. Parametric values of FA and MD were extracted using the previously transformed callosal segments in the native high resolution (T1w) space to avoid interpolation errors in transferring callosal segments to the low-resolution native diffusion space.

2.3.3. Magnetization transfer images

Magnetization transfer images with (MT_{on}) and without (MT_{off}) saturation pulse were stripped of non-brain tissue using *bet*, MT_{on} images were linearly aligned (brain-only, *flirt*, 6 dof) to MT_{off} images and magnetization transfer ratios (MTR) were calculated as (MT_{off} - MT_{on})/MT_{off}. The MTR maps were linearly (*flirt*, 6 dof) registered and transformed to the native T1w images. Based on visual inspection of ROIs, registration with six degrees of freedom (translation, rotation) was sufficient for intra-subject MTR-to-T1w registration. Callosal MTR was extracted using segments transformed to native T1w space as described above.

2.3.4. Relaxometry images (mcDESPOT)

Preprocessing for mcDESPOT (R1, R2 and MWF) data was conducted in Cardiff University Brain Research Imaging Centre. All images were co-registered linearly to the Spoiled Gradient Recalled (SPGR) image acquired with a flip-angle of 13° to correct for head motion. The images were stripped of non-brain tissue using *bet* algorithm. Registration and brain masking were performed with *FSL*. Using maps generated from the Inversion Recovery-SPGR and 2 phase-cycling Steady-State Free Precession (SSFP) acquisitions, images were then corrected for B1 inhomogeneities and off-resonance artefacts, respectively. The B1 and off-resonance inhomogeneities were modelled using the DESPOT1-HIFI (Deoni, 2007) and DESPOT2-FM (Deoni, 2009) models respectively, these were then input into the fitting of the mcDESPOT model. The mcDESPOT algorithm (Deoni et al., 2008) was used to identify the fast relaxing (water trapped within the myelin layers) and slow relaxing (free-moving water in intra- and extra-cellular space) components of the T1 and T2 decay and the corresponding volume fractions. The fast volume fraction, i.e. fast water component divided by total, was taken as a map of the myelin water fraction (MWF). Images in each mcDESPOT modality (T1, T2 and MWF) were individually registered (brain-only, *flirt*, 12 dof) to the native T1w image for extracting the segment-wise mean values. Nonlinear registration provided better alignment of callosal ROIs in parametric images (possibly due to higher field strength of 3T in ALSPAC).

The projected callosal segments were visually inspected in each MRI measure and erroneous projections were excluded. For a more detailed account on exclusion, see Supplementary Material.

2.4. Statistical analyses

Comparison of the exposed and non-exposed groups in continuous variables (Age, Birth weight and IQ) were performed using independent two-sample t-tests. Fisher's exact test was used for categorical variables (Maternal education level, Maternal alcohol use during pregnancy, Family income and Maternal drug use during pregnancy) and exclusion rate (quality control of T1w data registration).

Data extracted from the 10 callosal segments were analyzed in R (R Core Team, 2018). In MTR images acquired in SYS, outliers (±4 SD) were removed separately for two different acquisition schemes, after which the data were mean-centered by acquisition. Outliers (±3 SD) were removed by segment separately in each cohort, sex and imaging measure. Outlier in any segment prompted the removal of all data of the individual's affected MRI measure. Volumes of each of the 10 callosum segments were normalized by the individual's whole-brain volume. Relaxation rates R1 and R2 were calculated in the ALSPAC cohort. Finally, all MRI-derived callosal data were normalized (z-score) separately in each cohort, sex, imaging measure and callosal segment (removing by-segment variation) to facilitate comparisons across the exposure (Fig. 1).

As stated above, for callosal volume, FA, MD and MTR, the NFBC1986 was chosen as a discovery cohort and the SYS and ALSPAC as replication cohorts. In each cohort and for each MRI measure, the main effect of the exposure (PEMCS 0 or 1) on callosal segments (coded from 1 to 10, anterior to posterior) was evaluated using linear mixed-effects models. All 10 segments were placed in a single model in each cohort, sex and modality. In Model 1, participant Age was included as a fixed-effect confounding variable. In Model 2, fixed-effects included participant Age, Maternal education level, Maternal alcohol use during pregnancy and Family income and Maternal drug use during pregnancy (the latter two variables only in ALSPAC and SYS). In addition, we tested for Exposure-by-Sex and Exposure-by-Segment interactions in Model 2. As random effects in all tests, we included intercepts for individual and, in SYS, individual nested in sibship. Note that we did not include callosal segment as random effect because data were normalized by-segment (z-score), as stated above.

Pooled data of all callosal MRI measures were included in a mega-analysis using mixed-effects models separately in males and females. A separate model was constructed for each measure (callosal volume, MTR, FA and MD), enabling models that combine data from two or three cohorts according to the availability of callosal MRI measures. All mega-analyses included Model 1 (as above) and Model 2 (without Family income and Maternal drug use, as these were not available for the NFBC1986). Cohort was included as a random effect in all mega-analysis models.

In order to estimate statistical significance, models with and without the exposure were tested against each other using likelihood ratio tests. Comparison of models was implemented because mixed models do not provide a straightforward p-value (Winter, 2013). Multiple comparisons were controlled with false discovery rate (FDR) in each cohort and model (e.g. n = 4 for FDR in males in NFBC1986, Model 1). As *post hoc* analyses, multivariate linear models, controlling for the same covariates as in Model 2, were fitted by-segment in those MRI metrics that had shown Exposure-by-Segment interaction. A p-value less than 0.05 (after FDR correction) was considered significant. All analyses were performed separately for males and females in normalized callosal measures.

Relationship between MRI measures and participant Age was analyzed using inter-individual correlation (Pearson correlation coefficient) by callosal segment. Finally, mean correlation was calculated between Mean Diffusivity (MD) and other MRI measures across the callosum in the NFBC1986 and the ALSPAC.

3. Results

Demographic information for the three cohorts (ALSPAC, SYS and

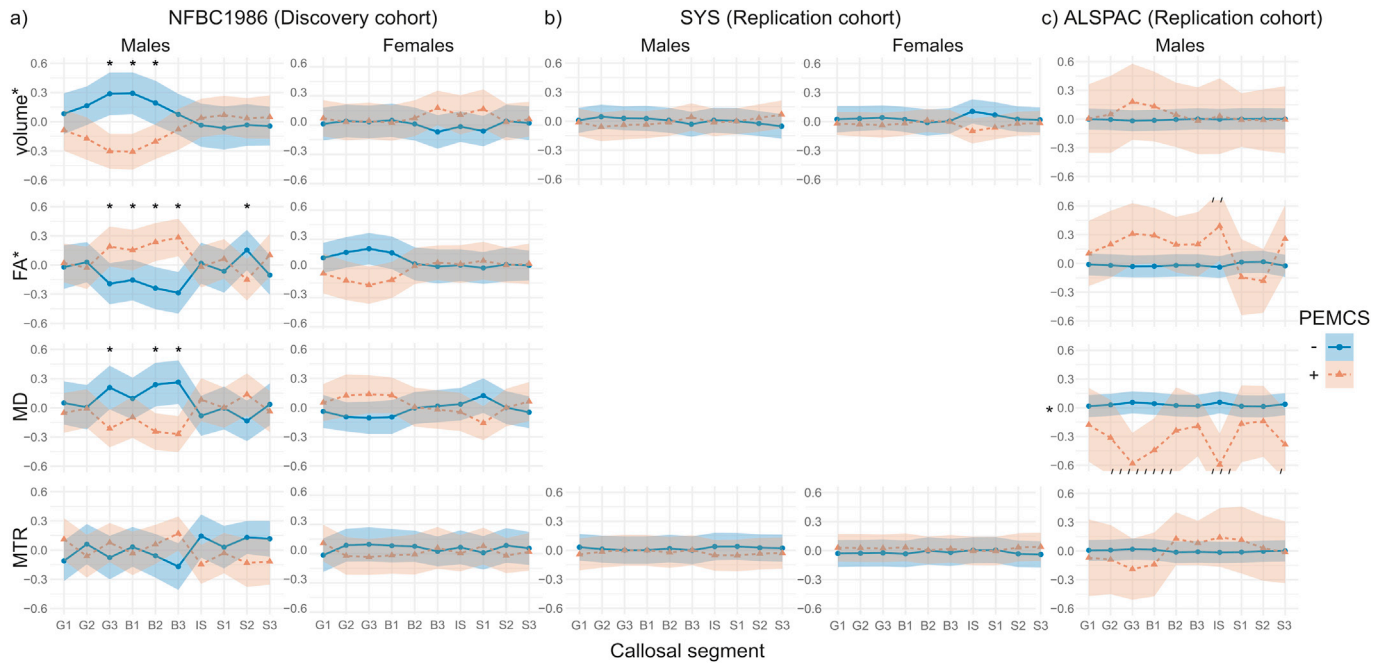

Fig. 1. Anterior-posterior profiles of normalized (z-score) callosal MRI measures in exposed (PEMCS, red) and non-exposed (blue) males and females in the Northern Finland Birth Cohort 1986 (NFBC1986 [a]), Saguenay Youth Study (SYS [b]) and in males in the Avon Longitudinal Study of Parents and Children (ALSPAC [c]). Associations between PEMCS and MRI measures were analyzed, first, by-measure using mixed-effects models and, second, by-segment in males in the NFBC1986 due to the observed Segment-by-Exposure interaction. MRI measures and individual callosal segments showing association with PEMCS are marked with asterisk (*) and detailed in Table 3 and Table S1, respectively. Colored 95% confidence intervals were cut at z-score 0.6 for visualization. Names of callosal segments: G, genu; B, body; IS, isthmus; S, splenium.

Table 2
Demographic information for the Saguenay youth Study (SYS), the Northern Finland Birth Cohort 1986 (NFBC1986) and the Avon Longitudinal Study of Parents and Children (ALSPAC).

	The NFBC1986 Study				The SYS Study				The ALSPAC Study	
	Males		Females		Males		Females		Males	
	Non-exposed	Exposed	Non-exposed	Exposed	Non-exposed	Exposed	Non-exposed	Exposed	Non-exposed	Exposed
Sample size	95	93	145	113	252	192	240	250	333	34
Age (years)	26.38 ± 0.46	26.49 ± 0.52	26.48 ± 0.54	26.41 ± 0.50	14.92 ± 1.78	14.97 ± 1.79	15.10 ± 1.91	15.10 ± 1.85	19.55 ± 0.81	19.77 ± 0.84
IQ	112.84 ± 17.96	103.98 ± 19.68 *	110.28 ± 19.08	110.18 ± 20.23	104.23 ± 12.68	104.62 ± 12.30	105.43 ± 11.46	103.51 ± 12.16	97.21 ± 12.27	93.81 ± 12.49
Birth weight (g)	3717.26 ± 461.12	3602.15 ± 491.92	3576.69 ± 450.62	3417.43 ± 451.95 *	3540.79 ± 471.96	3365.39 ± 475.12 *	3490.77 ± 459.21	3210.44 ± 473.45 *	3555.76 ± 513.84	3477.94 ± 471.58
Maternal education (%)		*r = 0.12*		*r = 0.00*		*r = 0.02*		*r = -0.15* *		*r = -0.19* *
level 1	46.32	36.56	29.66	31.86	18.25	16.67	12.50	19.60	8.41	17.65
level 2	18.95	15.05	17.24	15.93	34.13	36.98	31.25	43.20	29.13	52.94
level 3	25.26	36.56	34.48	30.09	32.94	28.65	36.67	20.40	34.23	20.59
level 4	9.47	11.83	18.62	22.12	14.68	17.71	19.58	16.80	28.23	8.82
Maternal alcohol use (%)	10.53	16.13	8.28	27.43 *	15.87	34.90 *	19.16	30.00 *	29.43	32.35
Family income (%)						*r = -0.06* *		*r = -0.07*		*r = -0.26* *
level 1	–	–	–	–	17.46	28.65	17.50	27.20	11.41	44.12
level 2	–	–	–	–	29.37	18.23	28.75	22.40	23.42	29.41
level 3	–	–	–	–	28.57	29.69	27.92	27.20	27.93	11.76
level 4	–	–	–	–	24.60	23.44	25.83	23.20	37.24	14.71
Maternal drug use (%)	–	–	–	–	0.00	0.01	0.00	0.00	0	2.94 *

*$p < 0.05$.
T-test was used for estimating the significance of the effect of exposure on Age, IQ and Birth weight.
Fisher's exact test was used for estimating the significance of the effect of exposure on Maternal education, Maternal alcohol use during pregnancy, Family income and Maternal drug use during pregnancy.

NFBC1986) is presented in Table 2.

There were no differences (Fisher's exact test) in the number of excluded exposed and non-exposed individuals in visual inspection of nonlinear registration (callosal ROI alignment in T1w images) or removal of outliers, see Supplementary material for details.

Associations between PEMCS and lower callosal volume and higher FA were observed in exposed males in the Discovery cohort (NFBC1986) when adjusting for confounders (Model 2: Age, Maternal education, Maternal alcohol use during pregnancy, Family income and Maternal drug use), Table 3 and Fig. 1. Neither of these associations was observed in the replication cohorts (SYS and ALSPAC). The mega-analysis of each callosal MRI measure showed lower MD in exposed males in a combined sample of males of the NFBC1986 and ALSPAC (MD not available in SYS), Table 4. All other results, with some being significant without replication, are reported in Supplementary Table 2.

Testing for Exposure-by-Sex interaction in the NFBC1986 revealed a differential effect of the exposure on males and females for FA (males r = 0.20 and females r = −0.12; $\chi^2(1) = 6.93$, p = 0.008) and segment volume (males r = −0.18 and females r = 0.08; $\chi^2(1) = 6.99$, p = 0.008), Fig. 1. Analysis of Exposure-by-Segment interaction revealed effects in males in the NFBC1986 for segment volume, FA, MD and MTR, Table S1. Further analysis of the Exposure-by-Segment interaction in males in the NFBC1986 revealed several associations between PEMCS and individual callosal segments. Multivariate linear models (adjusted as in Model 2) showed relations for segment volume (in G3: r = −0.55, B1: r = −0.57 and B2: r = −0.38), FA (in G3: r = 0.46, B1: r = 0.36, B2: r = 0.50, B3: r = 0.56 and S2: r = −0.32) and MD (in G3: r = −0.45, B2: r = −0.46 and B3: r = −0.47), Fig. 1.

Correlation analysis of participant Age and MRI measures provided weak correlations, with a highest value of 0.25 (Age - R1 in B2 segment in ALSPAC), Table S3. Relationship between Mean Diffusivity and other MRI measures was analyzed due to the observed association with the exposure and MD in the mega-analysis (NFBC1986 and ALSPAC). We observed negative correlations between MD and all other measures (i.e., segment volume, FA [both cohorts], and R1, R2 and MWF [ALSPAC]). MTR showed discrepant results between the two cohorts, Table S4.

4. Discussion

In this report, we investigated the association between prenatal exposure to maternal cigarette smoking and both the volume and microstructure of the offspring corpus callosum in three community-based cohorts. We observed associations between PEMCS and lower callosal volume and higher FA in exposed (vs. non-exposed) young males in the "discovery" (NFBC1986) cohort, Table 3 and Fig. 1 but these associations were not replicated in the SYS or ALSPAC. A mega-analysis revealed lower MD in exposed (vs. non-exposed) males in a combined sample of the NFBC1986 and the ALSPAC, Table 4.

As expected, we observed lower birth weight in males and females in SYS, and females in NFBC1986, Table 2. It has been observed previously that variation in birth weight associated with PEMCS may be more pronounced in females, as compared with males (Voigt et al., 2006). It must be also noted that the neurodevelopmental consequences of nicotine exposure (in rodents) already emerge at doses lower than growth-impairing levels (Ribary and Lichtensteiger, 1989; Navarro et al., 1989).

We observed lower callosal volume in relation to PEMCS in young adulthood in males (NFBC1986, mean age 26.44 y), but the finding was not replicated in younger males (in SYS, mean age 14.94 y, or ALSPAC, mean age 19.57 y), Table 3 and Fig. 1. Lower callosal volume, in general, may reflect lower degree of axonal myelination or reduced axon caliber or the overall lower number of axons; lower overall density of axons is an unlikely explanation (Aboitiz et al., 1992). Similar microstructural features may account for the lower MD (Concha, 2014; Song et al., 2003) in exposed (vs. non-exposed) males, observed in a mega-analysis of a combined dataset of the ALSPAC and the NFBC1986, Table 4. Lower

Table 3
Associations between PEMCS and callosal MRI measures in the Northern Finland Birth Cohort 1986 (NFBC1986, Discovery cohort), the Saguenay youth Study (SYS, Replication cohort) and the Avon Longitudinal Study of Parents and Children (ALSPAC, Replication cohort).

Measure	NFBC1986 (Discovery)								SYS (Replication)						ALSPAC (Replication)			
	Males				Females				Males				Females			Males		
	b	SE	χ^2	p	b	SE	χ^2	p	b	SE	χ^2	p	b	SE	χ^2	p	b	SE	χ^2	p
Model 1:																				
volume	−0.18	0.08	5.71	0.02	0.07	0.06	1.30	0.25	−0.01	0.06	0.02	0.88	−0.06	0.05	1.41	0.24	0.05	0.11	0.23	0.63
FA	0.18	0.08	4.66	0.03	−0.10	0.07	2.42	0.12									0.18	0.11	2.48	0.12
MD	−0.15	0.09	3.03	0.08	0.05	0.07	0.52	0.47									−0.34	0.13	7.39	0.01*
MTR	−0.02	0.10	0.03	0.85	−0.04	0.08	0.21	0.65	−0.03	0.10	0.09	0.76	0.02	0.10	0.05	0.82	−0.02	0.15	0.01	0.92
Model 2:																				
volume	−0.18	0.08	5.70	0.02*	0.08	0.07	1.60	0.21	−0.01	0.06	0.01	0.93	−0.05	0.06	0.95	0.33	0.04	0.11	0.12	0.73
FA	0.20	0.08	5.47	0.02*	−0.12	0.07	2.81	0.09									0.17	0.12	1.95	0.16
MD	−0.12	0.09	2.09	0.15	0.06	0.07	0.84	0.36									−0.39	0.13	8.51	0.00*
MTR	−0.04	0.10	0.17	0.68	−0.04	0.08	0.23	0.63	−0.01	0.11	0.02	0.90	0.01	0.10	0.02	0.90	−0.02	0.16	0.01	0.91

Model 1. Predictor: PEMCS, outcome: brain measure, confounders: Age.
Model 2. Predictor: PEMCS, outcome: brain measure, confounders: Age, Maternal education, Maternal alcohol use, Family income and Maternal drug use (the latter two in SYS and ALSPAC).
b, beta estimate (variation in MRI measure [SD] per exposure [0 or 1]).
SE, standard error.
χ^2, Chi-square of the effect of exposure on the model (likelihood ratio test).
p, uncorrected p-value for the effect of exposure on the model (likelihood ratio test).
*p < 0.05 after correction for multiple comparisons (FDR).

Table 4
Associations between PEMCS and MRI measures in a mega-analysis of all three cohorts.

Measure	Mega-analysis							
	Males				Females			
	b	SE	χ^2	p	b	SE	χ^2	p
Model 1								
volume	−0.03	0.06	0.28	0.59	−0.01	0.06	0.06	0.80
FA	0.18	0.11	2.74	0.10				
MD	−0.21	0.08	21.30	0.00*				
MTR	−0.02	0.07	0.06	0.80	0.00	0.07	0.00	1.00
Model 2'								
volume	−0.04	0.06	0.41	0.52	−0.01	0.06	0.01	0.92
FA	0.18	0.11	2.81	0.09				
MD	−0.20	0.07	16.81	0.00*				
MTR	−0.01	0.07	0.05	0.83	0.00	0.07	0.00	0.96

Model 1. Predictor: PEMCS, outcome: brain measure, confounders: Age.
Model 2'. Predictor: PEMCS, outcome: brain measure, confounders: Age, Maternal education, Maternal alcohol use. Please note that Family income and Maternal drug use were not included.
b, beta estimate (variation in MRI measure [SD] per exposure [0 or 1]).
SE, standard error.
χ^2, Chi-square of the effect of exposure on the model (likelihood ratio test).
p, uncorrected p-value for the effect of exposure on the model (likelihood ratio test).
*$p < 0.05$ after correction for multiple comparisons (FDR).

callosal volume and higher FA in early adulthood in exposed (vs. non-exposed) males (NFBC1986), together with the observation of lower MD in exposed (vs. non-exposed) males (mega-analysis), may relate to a higher fraction of small-caliber axons, as indicated by our earlier findings on the relation between axon caliber (assessed histologically) and FA (Björnholm et al., 2017). Caution must be taken, however, when interpreting findings in the diffusion measures due to a relatively large voxel size and a related partial-volume effect.

An Exposure-by-Sex interaction was present for segment volume (males: r = −0.18 and females: r = 0.08) and FA (males: r = 0.20 and females: r = −0.12) in the NFBC1986 cohort, suggesting different trajectories of the associations with PEMCS between the sexes in early adulthood. The lack of main effect of PEMCS in females may relate to the greater vulnerability of the female brain to insults during the postnatal (vs. prenatal) period or other processes distinct to those in males (Fitch et al., 1991a, 1991b). No associations were observed between PEMCS and MTR in any cohort, suggesting that myelination of axons (Sled, 2018) and/or axon diameter (Paus, 2010) is not moderated by the exposure, and also that any features accountable for the sex differences observed earlier in the NFBC1986 sample (Björnholm et al., 2017) are not associated with PEMCS. The possible effects of the exposure may be, however, too subtle to detect, especially in the presence of partial-volume effect in this measure, please see Table 1 for scan resolution.

An Exposure-by-Segment interaction was present for males in callosal volume, FA, MD and MTR in the NFBC1986 cohort, Table S1. The findings suggest that the differential effect of PEMCS along the anterior-posterior axis of corpus callosum may only appear later in early adulthood. Segments showing an association with PEMCS in *post hoc* analysis situate mostly between posterior Genu and posterior Body, a region with an intermediate profile of myelinated small and some large diameter axons (Aboitiz et al., 1992). The exact regional variation of the hypothesized sex-specific effect of PEMCS is, however, difficult to predict due to lack of earlier information.

The correlation between Age and callosal MRI measures provided weak correlations in all cohorts, which implies homogeneity of the samples in respect to maturational changes (observable in MRI), Table S3. The narrow age range in ALSPAC and NFBC1986 may explain this observation, while, in SYS, the maturational changes may be too subtle to be detected using this method. The Age - MRI measure correlation may also be higher in other brain regions than those studied in this work. Furthermore, due to the observed association between PEMCS and MD in the mega-analysis, we investigated the correlation between callosal MD and other MRI measures, Table S4. The correlation between MD and R2 was moderate (r = −0.44), possibly relating to the observed association with PEMCS in these measures, Table 3 and Table S2. No major differences were observed between the two cohorts (ALSPAC and NFBC1986) in these correlations.

The reported sex-specific variation in callosal structural measures may relate to PEMCS-induced alterations in the programming of brain development during the fetal period. While numerous factors may account for our findings, we speculate that PEMCS disrupts hormonal effects during fetal development, as reported in animal studies (Fitch et al., 1991b; Sarasin et al., 2003), resulting in higher fraction of small-caliber axons in adolescence and early adulthood (Paus and Toro, 2009), i.e. during the ongoing maturation of white matter (Lebel et al., 2008; Westlye et al., 2010). There are also numerous, while conflicting, interpretations of our findings concerning interhemispheric transfer of information and cognition (Hutchinson et al., 2009; Sui et al., 2018). Nevertheless, our findings do not allow for inference of causality or testing developmental hypothesis and the reports of a non-causal effect of PEMCS on later outcomes must be kept in mind (Gustavson et al., 2017; D'Onofrio et al., 2008).

A major limitation of this work is the lack of longitudinal data (preferably spanning infancy), which impedes the investigation of the timing of the emergence of any possible PEMCS-related alterations. Pertaining to our cross-sectional data, the effect of cohort cannot be separated from that of age and interpretations are thus limited. Furthermore, despite harmonization of data processing, cohort differences limit combining data and the results of the mega-analysis must be considered with caution. Large age differences (and the maturational changes expected to take place) strongly limit assumptions of replication in the two cohorts. Replication would also benefit of the presence of identical MRI modalities in all cohorts. Findings in the ALSPAC (replication cohort) must be interpreted keeping in mind that inclusion in this cohort was not based on PEMCS, no association between PEMCS and birth weight was observed, and that only 9% of the sample were exposed. Including more confounders, e.g. participants and/or parents genetic, psychiatric or neurological diagnoses, would potentially reveal previously unknown effectors. Finally, larger sample sizes would allow for more power to detect subtle alterations accountable to the exposure.

5. Conclusions

Prenatal exposure to maternal cigarette smoking was observed to

associate with lower (mean) diffusivity in the corpus callosum. Other structural differences between exposed and non-exposed offspring were found in individual cohorts but did not replicate. Future studies should elucidate the association between PEMCS-related white matter alterations and the emergence of neurodevelopmental and psychopathological conditions in a longitudinal study design.

Funding and disclosure

ALSPAC. We are extremely grateful to the families who took part in this study and the ALSPAC team, including midwifes, interviewers, computer and laboratory technicians, clerical workers, research scientists, volunteers, managers, receptionists and nurses. The UK Medical Research Council and the Wellcome Trust (Grant ref: 092,731) and the University of Bristol provide core support for ALSPAC. This paper was supported by grants from the National Institutes of Health (R01MH085772 to T. Paus). The content is solely the responsibility of the authors and does not necessarily represent the official views of the National Institutes of Health.

NFBC1986. The Northern Finland Birth Cohort 1986 is funded by University of Oulu, University Hospital of Oulu, Academy of Finland, Sigrid Juselius Foundation, European Commission (EURO-BLCS, Framework 5 award QLG1-CT-2000-01643), NIH/NIMH (5R01MH63706:02). This work has also been funded by Finnish Cultural Foundation (North Ostrobothnia Regional fund) and Jenny and Antti Wihuri Foundation.

Funding was also received from the University of Oulu Graduate School, Research Foundation of Psychiatry, Juho Vainio Foundation, Yrjö Jahnsson Foundation, Päivikki and Sakari Sohlberg Foundation and the Instrumentarium Science Foundation.

We thank the following individuals for their contributions in acquiring data for the SYS: Manon Bernard (database architect, The Hospital for Sick Children) and Helene Simard, MA, and her team of research assistants (Cégep de Jonquière). The Canadian Institutes of Health Research and the Heart and Stroke Foundation of Canada fund the SYS.

Declaration of competing interest

The authors declare no competing financial interests.

Acknowledgments

The authors wish to acknowledge CSC – IT Center for Science, Finland, for computational resources.

Appendix A. Supplementary data

Supplementary data to this article can be found online at https://doi.org/10.1016/j.neuroimage.2019.116477.

Author contributions

Björnholm L: Conceived and designed the analysis, Performed the analysis, Wrote the paper. Nikkinen J: Conceived and designed the analysis, Collected the data, Wrote the paper. Kiviniemi V: Collected the data, Wrote the paper. Niemelä S: Conceived and designed the analysis, Collected the data, Wrote the paper. Drakesmith M: Conceived and designed the analysis, Collected the data, Contributed data or analysis tools, Performed the analysis, Wrote the paper. Evans JC: Conceived and designed the analysis, Collected the data, Contributed data or analysis tools, Performed the analysis, Wrote the paper. Pike GB: Conceived and designed the analysis, Collected the data, Contributed data or analysis tools, Wrote the paper. Richer L: Conceived and designed the analysis, Collected the data, Wrote the paper. Pausova Z: Conceived and designed the analysis, Collected the data, Wrote the paper: Veijola J: Conceived and designed the analysis, Collected the data, Wrote the paper. Paus T: Conceived and designed the analysis, Collected the data, Wrote the paper.

References

Aboitiz, F., Scheibel, A.B., Fisher, R.S., Zaidel, E., 1992. Fiber composition of the human corpus callosum. Brain Res. 598, 143–153.
Albers, L., von Kries, R., Sobotzki, C., Gao, H.J., Buka, S.L., Clifton, V.L., et al., 2018. Differences in maternal smoking across successive pregnancies - dose-dependent relation to BMI z-score in the offspring: an individual patient data (IPD) meta-analysis. Obes. Rev. 19, 1248–1255.
Andersson, J.L.R., Sotiropoulos, S.N., 2016. An integrated approach to correction for off-resonance effects and subject movement in diffusion MR imaging. Neuroimage 125, 1063–1078.
Andersson, J.L., Jenkinson, M., Smith, S., 2007. Non-linear Registration, Aka Spatial Normalisation FMRIB Technical Report TR07JA2, vol. 2. FMRIB Analysis Group of the University of Oxford, pp. 1–21.
Andersson, J.L.R., Graham, M.S., Zsoldos, E., Sotiropoulos, S.N., 2016. Incorporating outlier detection and replacement into a non-parametric framework for movement and distortion correction of diffusion MR images. Neuroimage 141, 556–572.
Andersson, J.L.R., Graham, M.S., Drobnjak, I., Zhang, H., Filippini, N., Bastiani, M., 2017. Towards a comprehensive framework for movement and distortion correction of diffusion MR images: within volume movement. Neuroimage 152, 450–466.
Atluri, P., Fleck, M.W., Shen, Q., Mah, S.J., Stadfelt, D., Barnes, W., et al., 2001. Functional nicotinic acetylcholine receptor expression in stem and progenitor cells of the early embryonic mouse cerebral cortex. Dev. Biol. 240, 143–156.
Björnholm, L., Nikkinen, J., Kiviniemi, V., Nordström, T., Niemelä, S., Drakesmith, M., et al., 2017. Structural properties of the human corpus callosum: multimodal assessment and sex differences. Neuroimage 152, 108–118.
Boyd, A., Golding, J., Macleod, J., Lawlor, D.A., Fraser, A., Henderson, J., et al., 2013. Cohort profile: the 'children of the 90s'–the index offspring of the Avon longitudinal study of parents and children. Int. J. Epidemiol. 42, 111–127.
D'Onofrio, B.M., Turkheimer, E.N., Eaves, L.J., Corey, L.A., Berg, K., Solaas, M.H., et al., 2003. The role of the children of twins design in elucidating causal relations between parent characteristics and child outcomes. JCPP (J. Child Psychol. Psychiatry) 44, 1130–1144.
D'Onofrio, B.M., Van Hulle, C.A., Waldman, I.D., Rodgers, J.L., Harden, K.P., Rathouz, P.J., et al., 2008. Smoking during pregnancy and offspring externalizing problems: an exploration of genetic and environmental confounds. Dev. Psychopathol. 20, 139–164.
Concha, L., 2014 Sep 12. A macroscopic view of microstructure: using diffusion-weighted images to infer damage, repair, and plasticity of white matter. Neuroscience 276, 14–28. https://doi.org/10.1016/j.neuroscience.2013.09.004.
Deoni, S.C.L., 2007. High-resolution T1 mapping of the brain at 3T with driven equilibrium single pulse observation of T1 with high-speed incorporation of RF field inhomogeneities (DESPOT1-HIFI). J. Magn. Reson. Imaging 26, 1106–1111.
Deoni, S.C.L., 2009. Transverse relaxation time (T2) mapping in the brain with off-resonance correction using phase-cycled steady-state free precession imaging. J. Magn. Reson. Imaging 30, 411–417.
Deoni, S.C., Rutt, B.K., Arun, T., Pierpaoli, C., Jones, D.K., 2008. Gleaning multicomponent T1 and T2 information from steady-state imaging data. Magn. Reson. Med. 60, 1372–1387.
El Marroun, H., Schmidt, M.N., Franken, I.H., Jaddoe, V.W., Hofman, A., van der Lugt, A., et al., 2014. Prenatal tobacco exposure and brain morphology: a prospective study in young children. Neuropsychopharmacology 39, 792–800.
Ernst, M., Moolchan, E.T., Robinson, M.L., 2001. Behavioral and neural consequences of prenatal exposure to nicotine. J. Am. Acad. Child Adolesc. Psychiatry 40, 630–641.
Fitch, R.H., Cowell, P.E., Schrott, L.M., Denenberg, V.H., 1991. Corpus callosum: ovarian hormones and feminization. Brain Res. 542, 313–317.
Fitch, R.H., Cowell, P.E., Schrott, L.M., Denenberg, V.H., 1991. Corpus callosum: demasculinization via perinatal anti-androgen. Int. J. Dev. Neurosci. 9, 35–38.
Fraser, A., Macdonald-Wallis, C., Tilling, K., Boyd, A., Golding, J., Davey Smith, G., et al., 2013. Cohort profile: the Avon longitudinal study of parents and children: ALSPAC mothers cohort. Int. J. Epidemiol. 42, 97–110.
Fried, P.A., 1995. Prenatal exposure to marihuana and tobacco during infancy, early and middle childhood: effects and an attempt at synthesis. Arch. Toxicol Suppl. 17, 233–260.
Gustavson, K., Ystrom, E., Stoltenberg, C., Susser, E., Surén, P., Magnus, P., et al., 2017. Smoking in pregnancy and child ADHD. Pediatrics 139.
Hutchinson, A.D., Mathias, J.L., Jacobson, B.L., Ruzic, L., Bond, A.N., Banich, M.T., 2009. Relationship between intelligence and the size and composition of the corpus callosum. Exp. Brain Res. 192, 455–464.
Irfanoglu, M.O., Walker, L., Sarlls, J., Marenco, S., Pierpaoli, C., 2012. Effects of image distortions originating from susceptibility variations and concomitant fields on diffusion MRI tractography results. Neuroimage 61, 275–288.
Jacobsen, L.K., Picciotto, M.R., Heath, C.J., Frost, S.J., Tsou, K.A., Dwan, R.A., et al., 2007. Prenatal and adolescent exposure to tobacco smoke modulates the development of white matter microstructure. J. Neurosci. 27, 13491–13498.
Järvelin, M.R., Hartikainen-Sorri, A.L., Rantakallio, P., 1993. Labour induction policy in hospitals of different levels of specialisation. Br. J. Obstet. Gynaecol. 100, 310–315.
Jenkinson, M., Smith, S., 2001. A global optimisation method for robust affine registration of brain images. Med. Image Anal. 5, 143–156.

Källén, K., 2000. Maternal smoking during pregnancy and infant head circumference at birth. Early Hum. Dev. 58, 197–204.
Khairullah, A., Cousino Klein, L., Ingle, S.M., May, M.T., Whetzel, C.A., Susman, E.J., et al., 2014. Testosterone trajectories and reference ranges in a large longitudinal sample of male adolescents. PLoS One 9, e108838.
Lange, S., Probst, C., Rehm, J., Popova, S., 2018. National, regional, and global prevalence of smoking during pregnancy in the general population: a systematic review and meta-analysis. The Lancet Global Health 6, e769–e776.
Lauder, J.M., 1985. Roles for neurotransmitters in development: possible interaction with drugs during the fetal and neonatal periods. Prog. Clin. Biol. Res. 163C, 375–380.
Lebel, C., Walker, L., Leemans, A., Phillips, L., Beaulieu, C., 2008. Microstructural maturation of the human brain from childhood to adulthood. Neuroimage 40, 1044–1055.
Lee, K.W., Richmond, R., Hu, P., French, L., Shin, J., Bourdon, C., et al., 2015. Prenatal exposure to maternal cigarette smoking and DNA methylation: epigenome-wide association in a discovery sample of adolescents and replication in an independent cohort at birth through 17 years of age. Environ. Health Perspect. 123, 193–199.
Lichtensteiger, W., Schlumpf, M., 1985. Prenatal nicotine affects fetal testosterone and sexual dimorphism of saccharin preference. Pharmacol. Biochem. Behav. 23, 439–444.
Liu, J., Cohen, R.A., Gongvatana, A., Sheinkopf, S.J., Lester, B.M., 2011. Impact of prenatal exposure to cocaine and tobacco on diffusion tensor imaging and sensation seeking in adolescents. J. Pediatr. 159, 771â€–775.
Lotfipour, S., Ferguson, E., Leonard, G., Miettunen, J., Perron, M., Pike, G.B., et al., 2014. Maternal cigarette smoking during pregnancy predicts drug use via externalizing behavior in two community-based samples of adolescents. Addiction 109, 1718–1729.
Luck, W., Nau, H., Hansen, R., Steldinger, R., 1985. Extent of nicotine and cotinine transfer to the human fetus, placenta and amniotic fluid of smoking mothers. Dev. Pharmacol. Ther. 8, 384–395.
MacKay, A., Laule, C., Vavasour, I., Bjarnason, T., Kolind, S., Mädler, B., 2006. Insights into brain microstructure from the T2 distribution. Magn. Reson. Imaging 24, 515–525.
McConnell, S., Ghosh, A., Shatz, C., 1989. Subplate neurons pioneer the first axon pathway from the cerebral cortex. Science 245, 978–982.
Mori, S., Zhang, J., 2006. Principles of diffusion tensor imaging and its applications to basic neuroscience research. Neuron 51, 527–539.
Navarro, H.A., Seidler, F.J., Schwartz, R.D., Baker, F.E., Dobbins, S.S., Slotkin, T.A., 1989. Prenatal exposure to nicotine impairs nervous system development at a dose which does not affect viability or growth. Brain Res. Bull. 23, 187–192.
Oliff, H.S., Gallardo, K.A., 1999. The effect of nicotine on developing brain catecholamine systems. Front. Biosci. 4, D883–D897.
Paus, T., 2010. Growth of white matter in the adolescent brain: myelin or axon? Brain Cogn. 72, 26–35.
Paus, T., Toro, R., 2009. Could sex differences in white matter be explained by g ratio? Front. Neuroanat. 3.
Paus, T., Nawazkhan, I., Leonard, G., Perron, M., Pike, G.B., Pitiot, A., et al., 2008. Corpus callosum in adolescent offspring exposed prenatally to maternal cigarette smoking. Neuroimage 40, 435–441.
Pausova, Z., Paus, T., Abrahamowicz, M., Almerigi, J., Arbour, N., Bernard, M., et al., 2007. Genes, maternal smoking, and the offspring brain and body during adolescence: design of the Saguenay Youth Study. Hum. Brain Mapp. 28, 502–518.
Pausova, Z., Paus, T., Abrahamowicz, M., Bernard, M., Gaudet, D., Leonard, G., et al., 2017. Cohort profile: the Saguenay youth study (SYS). Int. J. Epidemiol. 46, e19.
R Core Team, 2018. R: A Language and Environment for Statistical Computing. R Foundation for Statistical Computing, Vienna, Austria.
Ribary, U., Lichtensteiger, W., 1989. Effects of acute and chronic prenatal nicotine treatment on central catecholamine systems of male and female rat fetuses and offspring. J. Pharmacol. Exp. Ther. 248, 786–792.
Roza, S.J., Verburg, B.O., Jaddoe, V.W.V., Hofman, A., Mackenbach, J.P., Steegers, E.A.P., et al., 2007. Effects of maternal smoking in pregnancy on prenatal brain development. The Generation R Study. Eur. J. Neurosci. 25, 611–617.
Sarasin, A., Schlumpf, M., Muller, M., Fleischmann, I., Lauber, M.E., Lichtensteiger, W., 2003. Adrenal-mediated rather than direct effects of nicotine as a basis of altered sex steroid synthesis in fetal and neonatal rat. Reprod. Toxicol. 17, 153–162.
Schmierer, K., Scaravilli, F., Altmann, D.R., Barker, G.J., Miller, D.H., 2004. Magnetization transfer ratio and myelin in postmortem multiple sclerosis brain. Ann. Neurol. 56, 407–415.
Sled, J.G., 2018. Modelling and interpretation of magnetization transfer imaging in the brain. Neuroimage 182, 128–135.
Slotkin, T.A., Greer, N., Faust, J., Cho, H., Seidler, F.J., 1986. Effects of maternal nicotine injections on brain development in the rat: ornithine decarboxylase activity, nucleic acids and proteins in discrete brain regions. Brain Res. Bull. 17, 41–50.
Slotkin, T.A., Orband-Miller, L., Queen, K.L., Whitmore, W.L., Seidler, F.J., 1987. Effects of prenatal nicotine exposure on biochemical development of rat brain regions: maternal drug infusions via osmotic minipumps. J. Pharmacol. Exp. Ther. 240, 602–611.
Song, S., Sun, S., Ju, W., Lin, S., Cross, A.H., Neufeld, A.H., 2003. Diffusion tensor imaging detects and differentiates axon and myelin degeneration in mouse optic nerve after retinal ischemia. Neuroimage 20, 1714–1722.
Sui, Y.V., Donaldson, J., Miles, L., Babb, J.S., Castellanos, F.X., Lazar, M., 2018. Diffusional kurtosis imaging of the corpus callosum in autism. Mol. Autism. 9, 62-6018-0245-1. eCollection 2018.
BET2: MR-Based Estimation of Brain, Skull and Scalp Surfaces, 2005. Eleventh annual meeting of the organization for human brain mapping, Toronto.
Toro, R., Leonard, G., Lerner, J.V., Lerner, R.M., Perron, M., Pike, G.B., et al., 2008. Prenatal exposure to maternal cigarette smoking and the adolescent cerebral cortex. Neuropsychopharmacology 33, 1019–1027.
Voigt, M., Hermanussen, M., Wittwer-Backofen, U., Fusch, C., Hesse, V., 2006. Sex-specific differences in birth weight due to maternal smoking during pregnancy. Eur. J. Pediatr. 165, 757–761.
Wakschlag, L.S., Pickett, K.E., Cook Jr., E., Benowitz, N.L., Leventhal, B.L., 2002. Maternal smoking during pregnancy and severe antisocial behavior in offspring: a review. Am. J. Public Health 92, 966–974.
Westlye, L.T., Walhovd, K.B., Dale, A.M., Bjornerud, A., Due-Tonnessen, P., Engvig, A., et al., 2010. Life-span changes of the human brain white matter: diffusion tensor imaging (DTI) and volumetry. Cerebr. Cortex 20, 2055–2068.
Winter, B., 2013. A Very Basic Tutorial for Performing Linear Mixed Effects Analyses arXiv preprint arXiv:1308.5499.
Yochum, C., Doherty-Lyon, S., Hoffman, C., Hossain, M.M., Zelikoff, J.T., Richardson, J.R., 2014. Prenatal cigarette smoke exposure causes hyperactivity and aggressive behavior: role of altered catecholamines and BDNF. Exp. Neurol. 254, 145–152.
Zheng, J.Q., Felder, M., Connor, J.A., Poo, M.M., 1994. Turning of nerve growth cones induced by neurotransmitters. Nature 368, 140–144.